

The pseudogap in hole-doped cuprates: possible insights from the Kondo effect

J. R. Cooper

*Cavendish Laboratory, Department of Physics, University of Cambridge,
J.J. Thomson Avenue, CB3 0HE, United Kingdom*

(Dated: October 31, 2021)

It is argued that the unusual “non-states-conserving” fermion density of states, deduced from the specific heat of several families of hole-doped cuprates, points towards interpretations of the pseudogap based on the suppression of a Kondo or heavy fermion-like density of states by antiferromagnetic spin fluctuations.

One of the outstanding problems in the field of cuprate superconductivity is the origin of the pseudogap (PG) in hole-doped cuprates. Many important experimental facts were summarized and discussed over 20 years ago [1]. Since then careful experiments have revealed anomalies in several other physical properties [2] but it is likely that these effects are smaller. For example it has been suggested [3] that the small [4] charge density wave (CDW) anomalies are caused by the pre-existing PG since they are driven by the Fermi arcs detected by angle-resolved photoemission spectroscopy (ARPES) [5]. Here we suggest that the PG might be caused by low energy antiferromagnetic (*af*) spin fluctuations causing a deep dip in a Kondo or heavy fermion-like density of states (DOS) at the Fermi energy E_F .

Specific heat studies by Loram and collaborators, [6, 7] and a first-order phenomenological analysis in terms of a “non-states-conserving” V-shaped fermion DOS [6], centered at E_F , in an otherwise flat band, as sketched in Fig. 1(a), gave considerable insight into the PG for hole-doped cuprates, such as $\text{YBa}_2\text{Cu}_3\text{O}_{6+x}$ (YBCO), $\text{Bi}_2\text{Sr}_2\text{CaCu}_2\text{O}_{8+x}$ (Bi2212) at different oxygen levels (x), and $\text{La}_{2-y}\text{Sr}_y\text{CuO}_4$ (LSCO) namely:

A. The PG energy (E_G) falls approximately linearly with p , the number of added holes per CuO_2 unit, as $J_{af}(1 - [p/p_{crit}])$, disappearing abruptly at $p_{crit} = 0.17$ - 0.19 [6]. Here $J_{af}/k_B = 1200$ - 1500 K, is similar to the *af* interaction $J_{af}/k_B = 1700$ K [8] in the corresponding parent insulator with $p = 0$ and k_B is Boltzmann’s constant.

B. For a wide range of p , plots of $S_e(T)$ vs. T , where $S_e(T)$ is the non-phonon, electronic contribution to the entropy, are approximately linear and parallel to each other, above a certain temperature (T), see e.g. Fig. 1(a) of [7] for $0.095 < p < 0.22$. Those with $p < p_{crit}$ are displaced downwards from the plot for $p = p_{crit}$ so have lower entropy at all T . This behavior is consistent with a recent comprehensive NMR paper [9]. There is no sign of the entropy “coming back” up to at least 250 K [7]. For fermions with an energy(E)-dependent DOS we expect $S_e(T) = CT\chi_s(T)$, where $\chi_s(T)$ is the spin susceptibility and C is a constant, because both depend on the number of states within the thermal window $|E - E_F| \lesssim 2k_B T$. Data for $T\chi_s(T)$ of Bi2212 show this

behavior up to 400 K, see Fig. 13(a) of [7], as do data for $\text{Y}_{0.8}\text{Ca}_{0.2}\text{Ba}_2\text{Cu}_3\text{O}_{6+x}$, also up to 400 K [10], when allowance is made for an x -independent Curie or Curie-Weiss term. A CDW- or superconductor-like DOS would not be “non-states-conserving” at higher T because extra states above and below the gap energy exactly compensate for the number of missing states in the gap.

C. Plots of $S_e(T_0)$ vs. p and $k_B T_0 \chi_s(T_0)$ vs. p at fixed temperatures T_0 show anomalously large increases of $\approx k_B$ and $0.3\mu_B^2$ per added hole respectively [7] where μ_B is the Bohr magneton. For $p > p_{crit}$ they peak near $p = 0.25$ before falling again, but this interesting result has only been established experimentally for LSCO.

D. A further interesting property is that p_{crit} seems to be determined by the product of J_{af} and the DOS at high energy [7]. While points A to C are consistent with the picture described here, point D is not, because here there is no relation between J_{af} in the parent compound and the DOS at energies $E \gg E_G$.

It is widely accepted that the Hubbard model describes the basic physics of the cuprates, e.g. [11] and references therein, but it has not been solved rigorously at low T and as far as we know does not account for points A to D above. Similar underlying physics occurs in the Friedel-Anderson model [12] and the Kondo effect [13, 14], where non-magnetic host metals such as Cu or Au are alloyed with a small concentration (c_{imp}) of magnetic elements such as Fe or Mn. For both Kondo alloys and heavy fermion compounds, the electronic specific heat coefficient, $\gamma \equiv dS_e/dT$, is strongly enhanced at low T . In Wilson’s solution of the Kondo problem [15], the spin susceptibility χ_s^{imp} from the impurities with spin 1/2 for $T \ll T_K$ the Kondo temperature, is given by $\chi_s^{imp} = c_{imp} \frac{(g\mu_B)^2 w}{4k_B T_K}$, where $g \simeq 2$ is the g -factor and $w = 0.4128$ is the Wilson number [14], while γ_{imp} at low T , is given by

$$\gamma_{imp} = c_{imp} \frac{\pi^2 k_B w}{6T_K} \quad (1)$$

and $\frac{\chi_s^{imp}}{\gamma_{imp}} = R_W = 2R_0$, in agreement with experiments on some Kondo alloys [14]. Here $R_0 = \frac{3\mu_B^2}{\pi^2 k_B^2}$ is the Wilson ratio for non- or weakly-interacting fermions.

For Bi2212, γ varies from 0.86 to 0.98 mJ/g-at/K²

for p between 0.095 and 0.22 [7], so from Eqn. 1, and taking c_{imp} to be the concentration of Cu atoms, $T_K = 875$ to 768 K. When the measured susceptibility of Bi2212, 1.1 to $1.3 \cdot 10^{-4}$ emu/mole-Bi2212 [7] for the above range of p , is corrected for core diamagnetism ($-1.95 \cdot 10^{-4}$ emu/mol-Bi2212 [16]) and Van Vleck orbital paramagnetism ($0.866 \cdot 10^{-4}$ emu/mol-Bi2212, using the Cu-O₂ plane value for YBCO [17]) $\chi_s = 2.18$ to $2.38 \cdot 10^{-4}$ emu/mol-Bi2212. This gives a Wilson ratio $\chi_s/\gamma = 1.29$ to $1.34 R_0$ for the above range of p . For YBCO, where there are some uncertainties from the Cu-O chain contribution, $\chi_s/\gamma \simeq 1.2R_0$ [7, 18]. So the experimental data is closer to R_0 rather than the Wilson value of $2R_0$. In the picture outlined here this could be because the energy of the Cu d level is not sufficiently far below E_F , and indeed experimentally $\chi_s/\gamma \simeq R_0$ for a number of heavy fermion compounds [14]. However we note that $\chi_s/\gamma \simeq R_0$ is also predicted at moderate doping by numerical treatments of the $t - J$ model [19] which is the limit of the 2D Hubbard model for large $d - d$ Coulomb repulsion U . Here we take $T_K = 800$ K throughout for simplicity. Such a large value of T_K does occur in dilute alloys, for example in AlMn where $T_K = 600$ K at low T falling to 470 K near room temperature because of thermal expansion and the strong volume dependence of T_K [20]. This fall in T_K reduces the T -dependence of $\chi_s(T)$ from the usual $1/(T + T_K)$ law found for many alloys with lower T_K and less thermal expansion.

In this paper we consider three localized d states, d^0 , d^1 and d^2 with occupancy 0, 1 and 2 described by the asymmetric single orbital Anderson model and corresponding to the $d_{x^2-y^2}$ orbital of Cu with 0, 1 and 2 electrons respectively. $|E_0|$ is the energy required to transfer an electron from the d^1 state to the Fermi level of the conduction electrons at E_F , while $-|E_0| + U > 0$ is the energy required to transfer an electron from E_F to the d^2 state. The d^0 state does not need to be considered explicitly and we assume that the other 8 Cu d -electrons do not participate in the Kondo effect. Figs. 1(b) and (c), taken from Fig. 5 of [21], shows the energy-dependent DOS for an isolated ion obtained by numerical renormalization group (NRG) calculations for this model for $E_0 = -U/2$, the symmetric case, and various asymmetric cases, $-E_0/\Delta = 4, 3$ and 2 . Here U , set equal to $4\pi\Delta$ in [21], is the on-site $d-d$ Coulomb repulsion, and Δ is the half energy-width of the d -level caused by hybridization with the conduction electrons. At even smaller values of $|E_0|$ [21] there is a gradual change from the Kondo to the mixed valence to the empty orbital regions.

The familiar triple peak structure in Fig.1(b) has two side peaks arising from the localized d -level and a peak near E_F from the Kondo resonance in the conduction electron band. As originally shown by Kondo [22] it is caused by the af exchange interaction $-2J_{imp}\underline{S}_{imp}\cdot\underline{s}_e$, with $J_{imp} < 0$, between the spin on the magnetic ion, \underline{S}_{imp} and the spin of a conduction electron \underline{s}_e . The S_{imp}^+

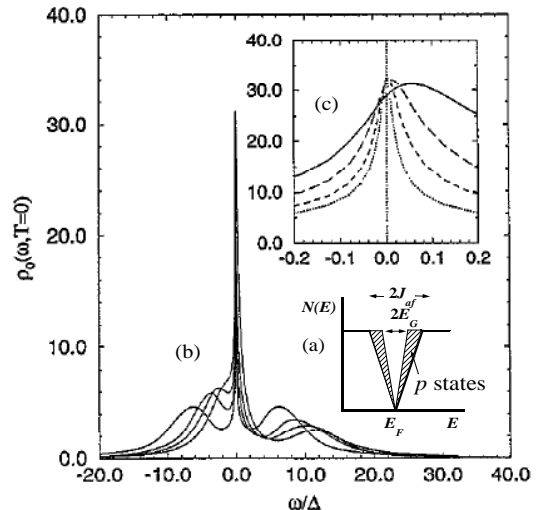


FIG. 1: (a) Fermion DOS used to rationalize specific heat data. (b) and (c), taken from [21] with permission, triple peak structure in the DOS $\rho(\omega)$ calculated using NRG theory for the single orbital, asymmetric Anderson model with $S_{imp} = 1/2$, for various values of $-E_0/\Delta = 2\pi, 4, 3$ and 2 . Here we estimate $E_0/\Delta = -3.08$ for the CuO₂ planes, so $\rho(\omega)$ is very close to the long-dashed curve (see text).

and S_{imp}^- operators do not commute, and because of this, higher order scattering processes contain the Fermi function for the conduction electrons. This leads to the logarithmic Kondo divergence in the scattering rate, which is responsible for the resistance minimum observed in dilute magnetic alloys and for the formation of the Kondo resonance at E_F . It is a many-body effect because it depends on the occupancy of many other conduction electron states. Table 1 of [21] lists quantities such as n_0 , the occupancy of the localized level and $k_B T_K/\Delta$ for various values of E_0/Δ . Δ is given by [12]:

$$\Delta = \pi V^2 N(E) \quad (2)$$

where V is the hybridization energy between the d state and the conduction electrons and $N(E)$ is their DOS for a given spin direction at the energy of the virtual bound state (vbs). Here any wave-vector dependence of V is ignored. For $3d$ impurities in copper V is 1-2 eV and Δ is typically 1 eV [12, 13]. We note that the Kondo resonance has the same spatial symmetry as the electronic state of the localized level [13, 23]. This is why band-structures of heavy fermion materials, calculated using relatively standard methods, agree with the extremal orbits observed in quantum oscillation experiments, e.g. [24], because the band structures depend on this symmetry. But the effective masses are larger, because they are determined by the energy width of the Kondo resonance. It is an important complement to Luttinger's theorem, which constrains the total volume of the

Fermi surface but not its shape. For the cuprates it implies that the Fermi surface is large and has the shape predicted by standard band theory even though the effective mass is larger.

The effects of an applied magnetic field (H) and, more generally, an exchange field, are important here. In dilute Kondo alloys, H suppresses the Kondo effect because spin-flip scattering processes become inelastic in a magnetic field [13]. Early tunnelling studies where a fraction of a monolayer of Fe atoms was evaporated on the oxide layer of an Al-Al₂O₃-Al junction [30] showed evidence for this “hole in the DOS” and it is indeed “non-states-conserving” (see Figs. 9 and 13 of [30]). Experimentally [31, 32] and theoretically [33, 34] this requires $\mu_B H \gtrsim k_B T_K$. So this precise picture cannot apply to the PG because a very large effective field, $\approx k_B T_K / \mu_B$, would be needed to give a deep PG, and this is incompatible with the small values of E_G inferred when $p \lesssim p_{crit}$.

This problem seems to be absent in NRG calculations [35] for the two-band Hubbard model, to which is added a ferromagnetic, predominantly Ising, exchange interaction $-2J_{ex} S_i^z \cdot s^z$ between the localized magnetic moments and the conduction electrons. Note that these calculations refer to a concentrated heavy fermion-like spin system. For $J_{ex} = 0$ there are two side peaks from the narrow band, i.e. the localized magnetic states, and a central peak from the broad band, equivalent to the conduction electron band here. But for $J_{ex} > 0$ there is a quadruple peak in some of the DOS curves, i.e. an extra dip at E_F , whose width is $\simeq 2J_{ex}$. It is possible that J_{ex} suppresses higher order spin-flip scattering processes, thereby suppressing the DOS at E_F . There appears to be no limitation regarding the ratio of $J_{ex}/k_B T_K$, in contrast to the effect of H on Kondo alloys.

The full-width-half-maximum (FWHM) of the central peak in Fig.1(c) is $2k_B T_K$ and as shown there, T_K varies strongly with E_0 . It also varies with U and Δ [21]. So the weak p dependence of γ and T_K for Bi2212 and other hole-doped cuprates, implies that the parameters E_0 , Δ and U are also only weakly dependent on p . In order to apply this picture to the cuprates we look at the conduction band that would be formed if the Cu d -electrons were well below the Fermi level. This has been done by calculating the band-structure of the hypothetical compound YBa₂Zn₃O₇, in which all lattice parameters are kept the same as for YBa₂Cu₃O₇, using the Wien2K code [25]. Fig. 2(b) shows dispersion curves for YBa₂Zn₃O₇, for the Brillouin zone sketched in Fig. 2(a). The Zn d -levels in the full d^{10} shell are well below E_F as shown more clearly by the the DOS *vs.* energy plots in Fig. 2(c) although in-plane states near E_F do have a small amount of $d_{x^2-y^2}$ character. In contrast, for YBa₂Cu₃O₇ the Cu $3d_{x^2-y^2}$ orbitals forming the Cu-O₂ plane bands are at higher energy. Fig. 2(c), also shows that the vbs and Kondo contributions to the total DOS are relatively small.

Fig. 1 of the Supplemental Material [26] shows pic-

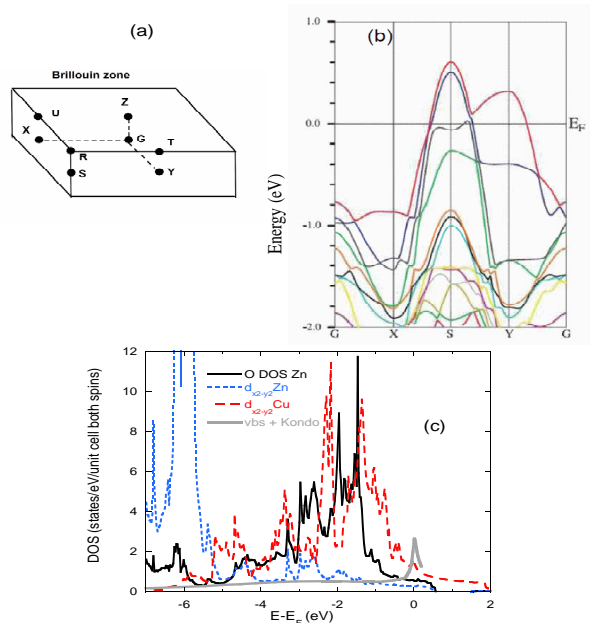


FIG. 2: Color online: (a) Brillouin zone showing symmetry points, (b) energy bands calculated for the hypothetical compound YBa₂Zn₃O₇, (c) partial DOS *vs.* energy E ; in-plane oxygen orbitals of YBa₂Zn₃O₇, solid black line, $d_{x^2-y^2}$ orbitals of YBa₂Zn₃O₇ and YBa₂Cu₃O₇ short and long dashed lines respectively, vbs and Kondo DOS from Figs. 1(b) and (c) for $\Delta = 1\text{eV}$ and $E_0 = -3\Delta$, solid grey line.

tures of the Fermi surface of YBa₂Zn₃O₇. There are two quasi-cylindrical sheets of a similar size extending along the k_z -axis, from the bands crossing E_F between S and X and between S and Y. One is extremely cylindrical, but the other changes from a circular to a rectangular section as k_z increases. The third band consists of an open surface, reminiscent of the chain band of YBa₂Cu₃O₇, from the curve crossing E_F between Y and G. The average value of E_F for the two quasi-cylindrical bands of the Zn compound is 0.54 eV relative to the top of the band, while the average value of k_F in the S-X-Y plane is $0.35 \pi/a$ where $a = 0.382 \text{ nm}$ is the in-plane lattice spacing. If both bands were precisely cylindrical the average number of occupied states (both spins) in each band would be given by $2\pi k_F^2 / (2\pi/a)^2 = 0.198$, i.e. 0.198 holes per CuO₂ unit which is remarkably close to experimental estimates [27–29]. In the simple two-cylinder approximation, if the Cu $3d$ -states are all well below E_F then $N(E_F) = 0.185 \text{ states/eV/Cu/spin}$. More precise values can be obtained from the DOS plots in Fig. 2(c), they give a hole concentration arising from the in-plane O_{xy} and Zn $d_{x^2-y^2}$ orbitals of $p = 0.185$ and $N(E_F) = 0.208 \text{ states/eV/Cu/spin}$, in good accord with the approximate estimates given above. It would be interesting to see whether this procedure works for the two-chain compound YBa₂Cu₄O₈.

It is difficult to estimate the hybridization parameter

V from the band structure of the host metal [14] for noble metal Kondo alloys and here it is even more complicated because of the complex band structure below ≈ -1 eV shown in Fig. 2(b). Therefore we set $\Delta = 1$ eV, a typical value for $3d$ impurities in noble metals [12, 13], giving $k_B T_K / \Delta = 0.054$, and we interpolate the data in [21], to find $E_0 = -3.08\Delta$. This corresponds to a Kondo DOS very close to the long-dashed line in Fig. 1(c). Note that the viability of this approach is only weakly affected by the precise value of Δ . If Δ were larger, but still much smaller than U , then $|E_0|$ would be larger, and the Kondo peak clearer, and even if Δ were as small as 0.12 eV, giving $T_K / \Delta = 0.59$ there would still be a Kondo resonance near E_F [21]. But uncertainty in the values of V and $N(E)$ in Eqn. 2 and in Δ is a potential weak point of our analysis.

The FWHM of the Kondo resonance is $2k_B T_K$ in energy. When transformed into \underline{k} - and then \underline{r} - space, and in the absence of a PG, n_K , the carrier density in the Kondo resonance, decays as $n_K \exp(-r/R)$ with a range $R = \frac{\hbar v_F}{k_B T_K}$. We find $n_K = 0.02$ states/Cu/spin for $-E_0 = 3.08\Delta$ from Lorentzian fits to the curves in Fig. 1(c) between -0.2Δ and E_F , suitably normalized to the peak at $-E_0 = U/2$ in Fig. 1(b), which contains approximately 1 electron. With $T_K = 800$ K and a Fermi velocity $v_F = 1.6 \cdot 10^7$ cm/sec, estimated for a cylindrical Fermi surface containing $1+p$ holes with an effective mass $5.2m_e$ [36], $R = 4a$. From the previous spatial symmetry argument, n_K will have $|d_{x^2-y^2}|$ symmetry and be larger in the (0,1) and (1,0) directions. In these directions af spin fluctuations cause neighboring spins to be anti-parallel over a certain spatial range, ξ . A typical value for $p = 0.1$ is $\xi = 0.9$ nm, i.e. $2-3a$ [8]. If $\xi = 2a$ then only the 4 nearest neighbors have correlated spins. Because of their af Kondo screening ‘‘clouds’’ they will give a *ferromagnetic* conduction electron spin polarization at the central site. When $|E_0| \gg \Delta$, the charge susceptibility is zero [14] and the spin polarization from the 4 neighbors will be $0.08 \exp(-1/4) \mu_B = 0.062 \mu_B$. It is difficult to prove that this spin polarization is equivalent to J_{ex} in [35], but, for $\chi_s = 2.3 \cdot 10^{-4}$ emu/mole-Bi2212, the field needed to produce a spin polarization of $0.062 \mu_B / \text{Cu}$ is $\mu_B H / k_B = 200$ K giving $J_{ex} / k_B = 400$ K. From Fig. 2 of [35] the total energy gap, equivalent to $2E_G$ here, is $2.2 J_{ex} / k_B \pm 25\% = 880 \pm 25\%$ K, reasonably close to the experimental value $2E_G / k_B = 1230$ K for $p = 0.1$. Note that the presence of the PG will reduce the spin polarization when $r \geq \frac{\hbar v_F}{E_G}$. Furthermore, the imaginary part of the self energy is unusual and typical of a ‘‘bad metal’’ [35] in agreement with experiments on the cuprates. However, more work is needed to see whether J_{ex} falls linearly with p and whether there can be asymmetry in the DOS about E_F on a scale of J_{ex} , i.e. E_G , that would account for the strong p -dependence of the measured thermoelectric power (TEP) and its scaling with $k_B T / E_G$ [18, 37].

Alternatively, in a related picture, the effect of the af fluctuations, i.e. the interactions between neighboring Cu spins, could be considered directly, without appealing to the work of Ref. [35]. These will reduce the entropy of the Cu spins and hence that available for the Kondo resonance. Key theoretical questions are (a) can they cause a deep PG even when the interaction energy (W) is much smaller than $k_B T_K$ and (b) does W fall linearly with p and become very small for $p \geq p_{crit}$? Experimental evidence for (b) is given by ratio of the ^{63}Cu and ^{17}O NMR relaxation rates T_1^{-1} [1] which is a measure of the strength of low frequency spin fluctuations for which the effect of the PG on χ_s cancels out. It does indeed fall linearly with p , approaching zero at p_{crit} . Analysis [39] of neutron scattering data shows the same decrease for af spin fluctuations of energy below 50 meV, so on the time scale of the Kondo resonance, with $k_B T_K = 69$ meV, they will provide a molecular field that is nearly static.

Within the usual localized picture W arises from superexchange via completely occupied or completely empty oxygen $2p$ states. For a band with Fermi energy E_F , we should consider Wannier functions that have a lifetime of order \hbar / E_F . E_F will increase with p , thereby reducing W , which could account for point (b) above. As sketched for example in Fig. 13 of [18], only those parts of the large Fermi surface spanned by the af wave vector $\underline{Q} \approx (\frac{\pi}{a}, \frac{\pi}{a})$, will be affected by af fluctuations. This accounts for the Fermi arcs, where $E_G = 0$, in agreement with ARPES [5] and STM [38] data. It will also cause a strong energy dependence of the scattering rate that is probably responsible for the TEP [18] and its scaling with $k_B T / E_G$ [18, 37]. For $p > p_{crit}$ the TEP is smaller and more metal-like, consistent with the weak asymmetry of the DOS about E_F shown in Fig. 1(c).

Evidence for an energy scale of $k_B T_K \simeq 70$ meV in the many spectroscopic studies of cuprates above T_c would be a good experimental test of the present picture. ARPES data do show structure on this energy scale but this is presently ascribed to other factors. For Kondo alloys STM studies [40] show asymmetry for positive and negative bias voltages arising from interference, a Fano effect, between the conduction electrons and the magnetic impurity, in contrast to planar tunnelling data [30]. Such asymmetry could be important when analyzing STM data for the cuprates [38]. Comprehensive studies of optical properties, reviewed for example in [41] and [42], provide a wealth of information but would need to be considered within a Kondo or heavy fermion-like picture. Another strong test would be recent work on the p -dependence of the T^1 term in the electrical resistivity of overdoped cuprates and its correlation with the superfluid density [43]. One prediction of the present approach is that the effective mass and related properties of overdoped Tl2201 crystals will be strongly pressure dependent since for classical Kondo alloys the volume (V) dependence of T_K is large, $-\ln T_K / \ln V = 16-18$ [20, 44].

So in summary, guided by the unusual behavior of the electronic entropy that is revealed by specific heat measurements [6, 7], we propose that the pseudogap in the energy scale over which a Kondo-like enhanced DOS at the Fermi energy is suppressed by *af* spin interactions.

The author would like to thank A. Carrington, who also calculated the band structure of $\text{YBa}_2\text{Zn}_3\text{O}_7$, J. L. Tallon and V. Zlatic for helpful suggestions and discussions and to acknowledge a long and happy collaboration with the late Dr. J. W. Loram.

-
- [1] J. L. Tallon and J. W. Loram, The doping dependence of T^* - what is the real high-T-c phase diagram? *Physica C-Superconductivity and its Applications* **349** 53-68 (2001).
- [2] B. Keimer, S. A. Kivelson, M. R. Norman, S. Uchida and J. Zaanen, From quantum matter to high-temperature superconductivity in copper oxides, *Nature* **519** 179-186 (2015).
- [3] R. Comin, A. Frano, M. M. Yee, Y. Yoshida, H. Eisaki, E. Schierle, E. Weschke, R. Sutarto, F. He, A. Soumyanarayanan, Y. He, M. Le Tacon, I. S. Elfimov, J. E. Hoffman, G. A. Sawatzky, B. Keimer, and A. Damascelli, Charge order driven by Fermi-arc instability in $\text{Bi}_2\text{Sr}_{2-x}\text{La}_x\text{CuO}_{6+\delta}$, *Science* **343**, 390-392 (2014).
- [4] I. Kokanovic and J. R. Cooper, Magnetic susceptibility of $\text{YBa}_2\text{Cu}_3\text{O}_{6+x}$ crystals: Unusual Curie behavior and small contributions from charge density waves, *Phys. Rev. B* **94** 075155-11 (2016).
- [5] S. Chen, M. Hashimoto, Y. He, D. Song, K.-J. Xu, J.-F. He, T. P. Devereaux, H. Eisaki, D.-H. Lu, J. Zaanen and Z.-X. Shen, Incoherent strange metal sharply bounded by a critical doping in $\text{Bi}2212$, *Science* **366**, 1099-1102 (2019).
- [6] J. W. Loram, K. A. Mirza, J. R. Cooper and J. L. Tallon, Specific heat evidence on the normal state pseudogap, *J. Phys. Chem. Solids* **59**, 2091-94 (1998).
- [7] J. W. Loram, J. Luo, J. R. Cooper, W. Y. Liang and J. L. Tallon, Evidence on the pseudogap and condensate from the electronic specific heat, *J. Phys. Chem. Solids* **62**, 59-64 (2001).
- [8] J. Rossat-Mignod, L. P. Regnault, C. Vettier, P. Bourges, P. Burllet, J. Bossy, J. Y. Henry and G. Lapertot, Spin dynamics in the high T_c system $\text{YBa}_2\text{Cu}_3\text{O}_{6+x}$, *Physica B* **180-181** 383-388 (1992).
- [9] J. Nachtigal, M. Avramovska, A. Erb, D. Pavicevic, R. Guehne and J. Haase, Temperature-independent cuprate pseudogap from planar oxygen NMR, *Condens. Matter* **5**, 66-84 (2020).
- [10] S. H. Naqib, J. R. Cooper, and J. W. Loram, Effects of Ca substitution and the pseudogap on the magnetic properties of $\text{Y}_{1-x}\text{Ca}_x\text{Ba}_2\text{Cu}_3\text{O}_{7-\delta}$, *Phys. Rev. B* **79**, 104519-8 (2009).
- [11] W. Wu, M. S. Scheurer, S. Chatterjee, S. Sachdev, A. Georges and M. Ferrero, Pseudogap and Fermi-surface topology in the two dimensional Hubbard model, *Phys. Rev. X* **8** 021048 (2018).
- [12] P. W. Anderson, Localized magnetic states in metals, *Phys. Rev.* **124**, 41 (1961).
- [13] G. Gruner Experimental evidence for many-body effects in dilute alloys, *Adv. Phys.* **23** 941-1023 (1974).
- [14] A. C. Hewson, "The Kondo problem to heavy fermions", Cambridge University Press, Cambridge, U.K. (1993).
- [15] K. G. Wilson, Renormalization group- critical phenomena and Kondo problem, *Rev. Mod. Phys.* **47** 773-840 (1975).
- [16] P. W. Selwood, "Magnetochemistry", Interscience Publishers (1964).
- [17] F. Mila and T. M. Rice, Analysis of magnetic resonance experiments in $\text{YBa}_2\text{Cu}_3\text{O}_7$, *Physica C* **157** 561-570 (1989).
- [18] J. R. Cooper and J. W. Loram, Some correlations between the thermodynamic and transport properties of high T_c oxides in the normal state, *J. Phys. I France* **6** 2237-2263 (1996).
- [19] J. Jaklic and P. Prelovsek, Finite-temperature properties of doped antiferromagnets, *Advances in Physics* **49** 1-92 (2000).
- [20] J. R. Cooper and M. Miljak, Single impurity behaviour and interaction effects in the magnetic susceptibility of AlMn and AlCr alloys, *J. Phys. F: Met. Phys.* **6** 2151-2164 (1976).
- [21] T. A. Costi, A. C. Hewson and V. Zlatic, Transport coefficients of the Anderson model via the numerical renormalization group, *J. Phys.: Condens. Matter* **6** 2519-2558 (1994).
- [22] J. Kondo, Resistance minimum in dilute magnetic alloys, *Prog. Theor. Phys.* **32** 37-49 (1964).
- [23] A. Blandin, Magnetic impurities in metals, *J. Appl. Phys.* **39** 1285-1294 (1968).
- [24] A. Pourret, M.-T. Suzuki, A. P. Morales, G. Seyfarth, G. Knebel, D. Aoki, and J. Flouquet, Fermi surfaces in the antiferromagnetic, paramagnetic and polarized paramagnetic states of CeRh_2Si_2 compared with quantum oscillation experiments, *J. Phys. Soc. Jpn.* **86**, 084702-7 (2017).
- [25] P. Blaha, K. Schwarz, G. K. H. Madsen, D. Kvasnicka and J. Luitz, "WIEN2K, An augmented plane wave + local orbitals program for calculating crystal properties", Karlheinz Schwarz, Techn. Universitt Wien, Austria, ISBN 3-9501031-1-2 (2001).
- [26] Supplemental material.
- [27] M. R. Presland, J. L. Tallon, R. G. Buckley, R. S. Liu and N. E. Flower, General trends in oxygen stoichiometry on T_c in Bi and Tl superconductors, *Physica C* **176** 95-105 (1991).
- [28] R. Liang, D. A. Bonn and W. N. Hardy, Evaluation of CuO_2 plane hole doping in $\text{YBa}_2\text{Cu}_3\text{O}_{6+x}$ single crystals, *Phys. Rev. B* **73** 180505-180508(R) (2006).
- [29] S. D. Obertelli, J. R. Cooper and J. L. Tallon, Systematics in the thermoelectric power of high T-c oxides, *Phys. Rev. B* **46** 14928(R) (1992).
- [30] S. Bermon, D. E. Paraskevopoulos and P. M. Tedrow, Ultra-high magnetic field study of the Kondo-type zero-bias conductance peak in magnetically doped metal-insulator-metal tunnel junctions, *Phys. Rev. B* **17** 2110-2123 (1978).
- [31] P. Monod, Magnetic field dependence of the Kondo resistivity minimum in CuFe and CuMn alloys, *Phys. Rev. Lett.* **19** 1113-1156 (1967).
- [32] H. Rohrer, High-field magnetoresistance of dilute Cu-Mn and Cu-Fe alloys, *Journ. Applied Phys.* **40**, 1472-1473 (1969).
- [33] B. Horvatic and V. Zlatic, Magnetic field effects for the asymmetric Anderson Hamiltonian, *Phys. Rev. B* **30**

- 6717-6731 (1984).
- [34] T. A. Costi, Kondo effect in a magnetic field and the magnetoresistivity of Kondo alloys, *Phys. Rev. Lett.* **85** 1504-1507 (2000).
- [35] T. A. Costi and A. Liebsch, Quantum phase transition in the two-band Hubbard model, *Phys. Rev. Lett.* **99** 236404-4 (2007).
- [36] A. F. Bangura, P. M. C. Rourke, T. M. Benseman, M. Matusiak, J. R. Cooper, N. E. Hussey, and A. Carrington, Fermi surface and electronic homogeneity of the overdoped cuprate superconductor $Tl_2Ba_2CuO_{6+\delta}$ as revealed by quantum oscillations, *Phys. Rev. B* **82** 140501(R) (2010).
- [37] J. R. Cooper, H. Minami, V. W. Wittorff, D. Babić and J. W. Loram, Effect of the normal state gap on the thermoelectric power, irreversibility line and c-axis resistivity of $YBa_2Cu_3O_{7-\delta}$, *Physica C* **341** 855-858 (2000).
- [38] K. Fujita, C. K. Kim, I. Lee, J. Lee, M. H. Hamidian, I. A. Firmo, S. Mukhopadhyay, H. Eisaki, S. Uchida, M. J. Lawler, E.-A. Kim and J. C. Davis, Simultaneous transitions in cuprate momentum-space topology and electronic symmetry breaking, *Science* **344** 612-616 (2014).
- [39] J. G. Storey, J. L. Tallon and G. V. M. Williams, Pseudogap ground state in high temperature superconductors, *Phys. Rev. B* **78** 140506(R) (2008).
- [40] V. Madhavan, W. Chen, T. Jamneala, M. F. Crommie and N. S. Wingreen, Tunneling into a single magnetic atom: spectroscopic evidence of the Kondo resonance, *Science* **280** 567 (1998).
- [41] D. N. Basov and T. Timusk, Electrodynamics of high- T_c superconductors, *Rev. Mod. Phys.* **77** 721 (2005).
- [42] S. Tajima, Optical studies of high-temperature superconducting cuprates, *Rep. Prog. Phys.* **79** 094001 (2016).
- [43] M. Čulo, C. Duffy, J. Ayres, M. Berben, Y.-T. Hsu, R. D. H. Hinlopen, B. Bernáth and N. E. Hussey, Possible superconductivity from incoherent carriers in overdoped cuprates, *SciPost Phys.* **11**, 012 (2021).
- [44] J. S. Schilling and W. B. Holzapfel, Effect of pressure on the Kondo temperature of Cu:Fe-existence of a universal resistivity curve, *Phys. Rev. B* **8** 1216-1237 (1973).

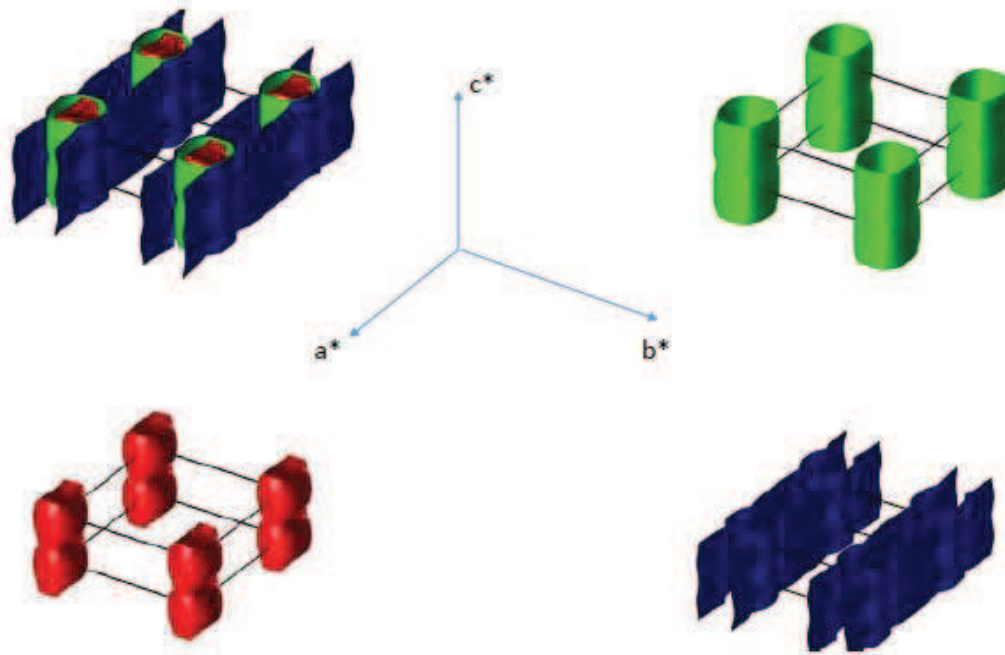


Figure 1, Color on line. Calculated Fermi surface (FS) for the hypothetical compound $\text{YBa}_2\text{Zn}_3\text{O}_7$. Clockwise from top left: full FS, quasi-cylindrical sheet, open sheet and distorted cylindrical sheet. Directions in reciprocal space are shown.